JOURNAL OF BACTERIOLOGY, Feb. 2007, p. 691–705 Vol. 189, No. 3
0021-9193/07/$08.00+0 doi:10.1128/JB.00921-06

Morphogenesis of the *Bacillus anthracis* Spore▽

Rebecca Giorno,[1] Joel Bozue,[2] Christopher Cote,[2] Theresa Wenzel,[1] Krishna-Sulayman Moody,[2] Michael Mallozzi,[1] Matthew Ryan,[1] Rong Wang,[3] Ryszard Zielke,[4] Janine R. Maddock,[4] Arthur Friedlander,[5] Susan Welkos,[2] and Adam Driks[1]*

Department of Microbiology and Immunology, Loyola University Medical Center, Maywood, Illinois 60153[1]; Bacteriology Division, United States Army Medical Research Institute of Infectious Diseases, Fort Detrick, Frederick, Maryland 21702-5011[2]; Department of Biological, Chemical, and Physical Sciences, Illinois Institute of Technology, Chicago, Illinois 60616[3]; Department of Molecular, Cellular, and Developmental Biology, University of Michigan, Ann Arbor, Michigan 48109[4]; and Headquarters, United States Army Medical Research Institute of Infectious Diseases, Fort Detrick, Frederick, Maryland 21702-5011[5]

Received 26 June 2006/Accepted 1 November 2006

***Bacillus* spp. and *Clostridium* spp. form a specialized cell type, called a spore, during a multistep differentiation process that is initiated in response to starvation. Spores are protected by a morphologically complex protein coat. The *Bacillus anthracis* coat is of particular interest because the spore is the infective particle of anthrax. We determined the roles of several *B. anthracis* orthologues of *Bacillus subtilis* coat protein genes in spore assembly and virulence. One of these, *cotE*, has a striking function in *B. anthracis*: it guides the assembly of the exosporium, an outer structure encasing *B. anthracis* but not *B. subtilis* spores. However, CotE has only a modest role in coat protein assembly, in contrast to the *B. subtilis* orthologue. *cotE* mutant spores are fully virulent in animal models, indicating that the exosporium is dispensable for infection, at least in the context of a *cotE* mutation. This has implications for both the pathophysiology of the disease and next-generation therapeutics. CotH, which directs the assembly of an important subset of coat proteins in *B. subtilis*, also directs coat protein deposition in *B. anthracis*. Additionally, however, in *B. anthracis*, CotH effects germination; in its absence, more spores germinate than in the wild type. We also found that SpoIVA has a critical role in directing the assembly of the coat and exosporium to an area around the forespore. This function is very similar to that of the *B. subtilis* orthologue, which directs the assembly of the coat to the forespore. These results show that while *B. anthracis* and *B. subtilis* rely on a core of conserved morphogenetic proteins to guide coat formation, these proteins may also be important for species-specific differences in coat morphology. We further hypothesize that variations in conserved morphogenetic coat proteins may play roles in taxonomic variation among species.**

A central problem in cell biology is understanding how cellular structures assemble. A well-established model for addressing this problem is the formation of specialized dormant cells, called spores, produced by *Bacillus* spp. and *Clostridium* spp. as a response to nutrient limitation (77). This process, called sporulation, involves significant restructuring of the cellular architecture. Early in sporulation, an asymmetrically placed septum divides the cell into a small forespore and a larger mother cell compartment. Later, the forespore becomes encased in a series of proteinaceous protective layers known as the coat, which is made up of mother-cell-synthesized proteins (19, 23, 24). The number and morphological complexity of the coat layers vary significantly between species (1, 16, 18, 34, 86). The *Bacillus subtilis* coat is a relatively thick structure with two major layers: a darkly staining outer layer and a lighter-staining inner layer (1, 86). In contrast, the *Bacillus anthracis* coat appears thin and compact (Fig. 1A and B). Nonetheless, it possesses two morphologically distinct layers (1). The degree to which these correspond to the inner and outer layers in *B. subtilis* is unknown. Unlike *B. subtilis*, in *B. anthracis*, *Bacillus megaterium*, and other species, the spore is surrounded by an additional structure called the exosporium (28) and is separated from the coat by a region that we refer to as the interspace (Fig. 1A and B). When the spore encounters nutrients, it breaks dormancy and germinates. As germination proceeds, the spore swells, the coat unfolds and cracks open, and the newly metabolizing cell initiates vegetative growth (55, 72, 74).

Coat assembly is a complex multistep process (19, 32). In *B. subtilis*, for which coat assembly has been well studied, a critical early event in coat assembly is the localization of SpoIVA to the mother cell side of the forespore (20, 63, 64, 70, 79) (Fig. 2A). SpoIVA deposition marks the forespore exterior as the site of all future coat protein assembly. Next, a shell of coat proteins (called the precoat) assembles around SpoIVA. The outermost shell of the precoat harbors the coat protein CotE (20) (Fig. 2B). In the final stage, the inner and outer coat layers appear (Fig. 2C). The inner coat proteins deposit between the shells of SpoIVA and CotE, resulting in a striking lamella-like morphology. The outer coat forms around the shell of CotE. CotE is essential for outer coat assembly, as it interacts with most or all the outer coat proteins as well as proteins that connect it to the forespore (Fig. 2D), a total of at least 24 proteins (4, 39, 48, 94).

* Corresponding author. Mailing address: Department of Microbiology and Immunology, Loyola University Medical Center, 2160 South First Avenue, Bldg. 105, Rm. 3820, Maywood, IL 60153. Phone: (708) 216-3706. Fax: (708) 216-9574. E-mail: adriks@lumc.edu.
▽ Published ahead of print on 17 November 2006.

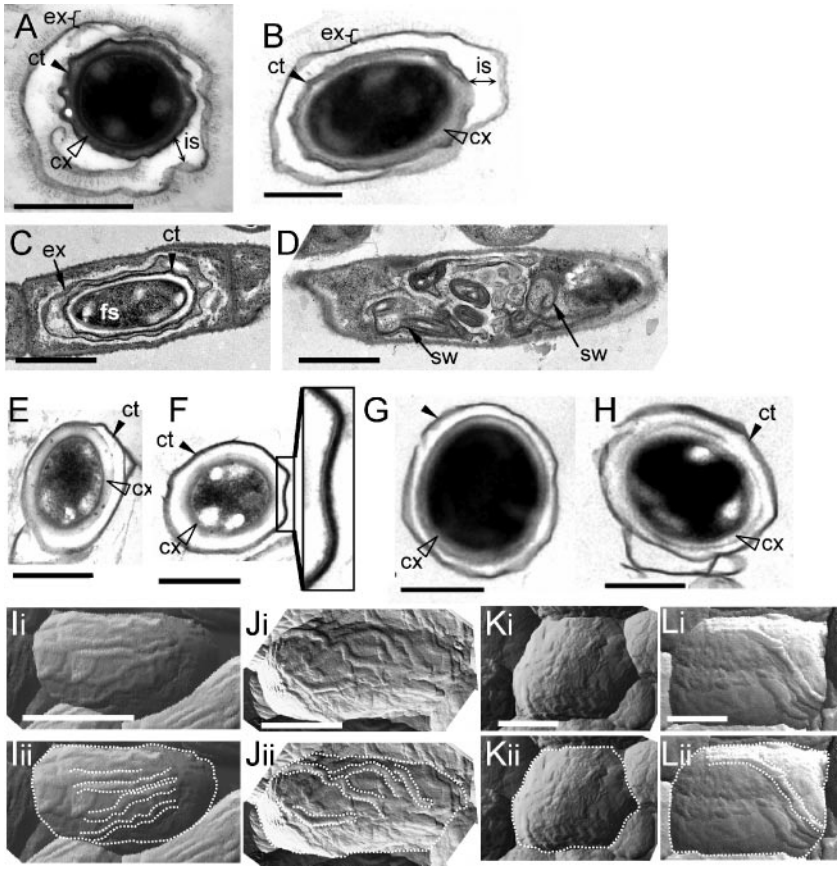

FIG. 1. Ultrastructural analysis of mutant sporangia and spores. Wild-type (A, B, C, and I), *spoIVA* (D), *cotE* (E, F, G, H, J, and K), or *cotH* (L) mutant sporangia or spores were analyzed by thin-section electron microscopy (A to H) or atomic force microscopy in the tapping mode (I to L). The inset in panel F shows an arc of the coat at a higher magnification in which the inner and outer coat layers are visible. Sterne wild-type (strain RG1) (A and I), *cotE* mutant (strain RG56) (E and F and J and K), and *cotH* mutant (strain RG7) (L) or Ames wild-type (B and C), *spoIVA* mutant (strain JAB11) (D), and *cotE* mutant (strain JAB4) (G and H) strain cells are shown. The bars indicate 500 nm (A, B, E to H, and J), 1 μm (C and D), 1.2 μm (I), 750 nm (K), and 840 nm (L). The closed arrowheads indicate the coat (ct), the open arrowheads indicate the cortex (cx), the brackets indicate the exosporium (ex), the double-headed arrows indicate the interspace (is), the forespore is indicated (fs), and arrows indicate exosporium (ex) or swirls of coat and exosporium material (sw) in sporangia. The white dotted lines (panels Iii, Jii, Kii, and Lii) indicate spore outlines as well as surface ridges.

In *B. subtilis*, several CotE-controlled proteins themselves direct the assembly of smaller subsets of coat proteins. One of these, CotH, directs the deposition of at least seven proteins (Fig. 2D) (39, 48, 57, 95). Interestingly, only 22% of the over 60 *B. subtilis* coat proteins (44, 46) have roles in assembly beyond their own deposition (19, 21, 32, 33). These so-called morphogenetic proteins are among the most highly conserved coat proteins between species (18). Morphogenetic coat proteins do not affect gene expression as far as is known (19, 32, 83). Instead, they work at the level of coat protein deposition or direct subsequent events like cross-linking.

The significant differences between *Bacillus* spp. in coat and exosporium morphology and the high degree of conservation of morphogenetic coat protein genes raise the question of how spore assembly programs among species have diverged to generate variations in spore ultrastructure and function. A critical aspect of this question is the role of the conserved morphogenetic coat proteins. Functional analysis of these genes in a variety of species should provide significant insight into how programs of cellular assembly evolve.

Here, we characterize *B. anthracis* homologues of *B. subtilis* morphogenetic coat proteins. *B. anthracis* coat assembly is of particular interest in anthrax pathogenesis. Studies of *B. subtilis* strongly argue that the coat (but not necessarily any individual coat protein) will play an essential role in *B. anthracis* spore resistance and in germination, both of which are needed for disease (16, 18, 19, 32, 75). Coat proteins are also likely to be useful as vaccine candidates (9, 13, 49, 90) and ligands for biological weapon detectors (10, 84, 92). Proteins to be used for these purposes should be required for virulence; otherwise, a determined enemy might prepare spores that are missing these proteins. In light of this, an especially critical open question is the possible role, if any, of the exosporium in virulence. This has not yet been tested using a virulent *B. anthracis* strain. However, an important study by Sylvestre et al. (80) showed the dispensability of a major exosporium protein, BclA, in an infection model that uses the attenuated Sterne strain (which lacks the capsule, a critical virulence factor) (22) and an immunocompromised mouse. BclA is the major structural component of the fringe of hair-like projections present on the

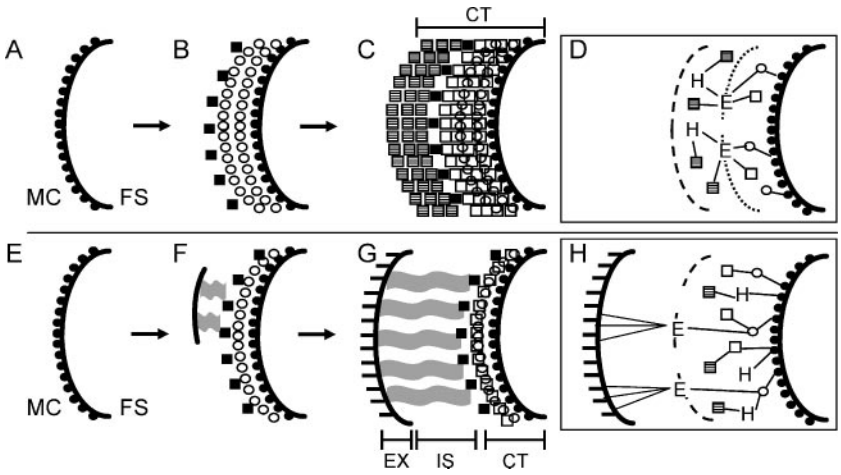

FIG. 2. Models for coat assembly in *B. subtilis* and *B. anthracis*. Panels A to H show arcs of the forespore surface. The incremental addition of structures on the forespore membranes during coat assembly in *B. subtilis* (A to C) and *B. anthracis* (E to G) and interactions between coat proteins in *B. subtilis* (D) and *B. anthracis* (H) are illustrated. The right-hand-most black arc in each panel indicates the outer forespore membranes, and the dashed arc in panels D and H indicates the outer coat surface. The solid circles at the outer forespore surface indicate the shell of SpoIVA, and the solid squares (in B, C, F, and G) represent CotE. CotE is represented by "E" and CotH is represented by "H" in panels D and H. MC, FS, CT, EX, and IS indicate mother cell, forespore, coat, exosporium, and interspace, respectively. See the text for further details.

exosporium basal layer (78, 80, 81). Therefore, in this model, BclA is not needed for disease. The role of any given coat protein in virulence is also unknown; while some degree of coat formation is undoubtedly required for anthrax, at least some individual proteins are likely to be dispensable.

We find that in spite of the large percentage of conserved coat proteins, coat assembly differs significantly between *B. subtilis* and *B. anthracis*. To a large degree, this is because important conserved morphogenetic proteins function in strikingly different ways in the two species. Mutations in morphogenetic protein genes may therefore be particularly important in the evolution of species-specific features of spores and their adaptation to novel niches. In addition, we find that the exosporium, the outermost structure of the *B. anthracis* spore, is dispensable for virulence in both intramuscular and intranasal challenge models. Therefore, an individual who might prepare *B. anthracis* as a biological weapon has the option of generating spores with or without an exosporium. As a result, we argue that proteins in both the coat and the exosporium should be considered for the use of vaccines or detector ligands.

MATERIALS AND METHODS

General methods. The Sterne strain was grown vegetatively in LB or brain heart infusion (BHI) medium (Difco) supplemented with 0.5% glycerol and induced to sporulate as described previously (46), unless otherwise noted. The onset of sporulation was defined as the first point at which the culture left exponential growth. Antibiotics were used when appropriate at the following concentrations: 75 μg/ml ampicillin, 5 μg/ml tetracycline, 5 μg/ml erythromycin, and 30 μg/ml (*Escherichia coli*) or 20 μg/ml (*B. anthracis*) kanamycin.

Ames strain vegetative cultures were grown in LB broth, and spores were prepared as previously described (36) by using Leighton-Doi medium (47) or Difco sporulation agar (73). Spores were then purified by centrifugation through a Hypaque-76 gradient (Nycomed, Inc., Princeton, NJ). Prior to use, spores were heated at 65°C for 30 min and then kept on ice.

Strains and plasmids used in this study are described in Table 1. Primer sequences are available upon request. Recombinant DNA procedures and chromosomal DNA isolation were performed according to methods described previously by Sambrook et al. (71) and Cutting and Vander Horn (14), respectively. Coat protein extraction and sodium dodecyl sulfate (SDS)-polyacrylamide gel electrophoresis (PAGE) analysis were performed as described previously (48). Sporangial lysates were prepared from 1 ml of a sporulating culture according to a method described previously (11). Western blot analysis was performed as described previously (4) using *B. subtilis* SpoIVA antiserum and *B. anthracis* CotE antiserum (see below). Electron and atomic force microscopy (AFM) were performed according to methods described previously by Catalano et al. (11) and Chada et al. (12), respectively. The calcium release assay was carried out according to a method described previously (87), except that spores were cultured on solid modified G medium (15 g/liter agar) for 3 to 5 days and germinated on AAC medium (89). Fluorescent dye uptake, heat sensitivity, and lysozyme sensitivity assays were carried out according to methods described previously by Welkos et al. (89), Bozue et al. (8), and Cutting and Vander Horn (14), respectively. The tetrazolium overlay assay was performed as described previously (14), except that the medium used to induce germination was supplemented with L-alanine (1.7 g/liter instead of 1 g/liter for *B. subtilis*), Casamino Acids (0.4 g/liter), and adenosine (1.7 g/liter).

To measure the germination of spores by the appearance of heat sensitivity, we generated spores by culturing them in Leighton-Doi medium, suspended them in BHI broth at a concentration of 10^7 spores/ml, and incubated them at 37°C with shaking at 150 rpm. At 15-min intervals, aliquots were removed, centrifuged, and resuspended in H_2O. CFU before and after heat treatment (65°C for 30 min) were then determined.

Phase-contrast microscopic examination of germination. Water-washed, heat-activated spores were suspended in water to a final optical density at 600 nm of 5.0. Twenty microliters of the spore suspension was spotted onto a slide that was first treated with 0.1% (wt/vol) poly-L-lysine. After 10 min of incubation, the remaining liquid was aspirated, nonadherent spores were removed by two water washes with 20 μl of water, and the sample was allowed to dry. To initiate germination, 5 μl of AAC medium was spotted onto the slide, followed by the placement of an 18-mm by 18-mm coverslip over the drop. Phase-contrast microscopy was performed using a Nikon Labophot microscope. Spores from three independent sporulations were scored as phase bright or phase dark for each strain at each time point. One hundred to 300 spores were counted for each time point. To prevent drying, slides were placed in a humid chamber between observations. The experiment was carried out at room temperature. The percentage of germination was calculated as follows: (total number of spores − number of phase-bright spores)/total number of spores.

Creation of *B. anthracis* mutants. Sterne and Ames strain mutants were generated using approaches based on methods described previously by Koehler et al. (41) and Mendelson et al. (53), respectively. To generate insertion-deletion mutations in the Sterne strain, we first constructed plasmid pMR1. To do this, a DNA fragment bearing the ΩKm-2 kanamycin resistance cassette generated by digesting plasmid pUC4ΩKm-2 (62) with BamHI was isolated and ligated into plasmid pSL1180 (Strategene) digested with BglII, resulting in plasmid pES1.

TABLE 1. Strains and plasmids used in this study

Strain or plasmid	Genotype or description	Source or reference
Strains		
Sterne strain derivatives		
RG1	Wild-type 34F2	P. Jackson
RG35	*cotB*Δ::Km	This study
RG56	*cotE*Δ::Km	This study
RG73	*cotH*Δ::Km	This study
RG154	*spoIVA*ΩpRG23	This study
Ames strain derivatives		
Ames	Virulent strain containing pXO1 and pXO2	49
JAB2	*cotB*ΩpKSM1	This study
JAB3	*cotH*ΩpKSM2	This study
JAB4	*cotE*ΩpKSM3	This study
JAB11	*spoIVA*::Km	This study
Other bacilli		
ADL18	*Bacillus subtilis* PY79	93
ADL830	*Bacillus cereus* T	A. Aronson
ADL831	*Bacillus cereus* 569	A. Aronson
ADL1390	*Bacillus subtilis*	69
ADL1391	*Bacillus pumilis*	69
ADL1392	*Bacillus licheniformis*	69
ADL1467	*Bacillus subtilis* natto	Laboratory collection
E. coli		
DH5α	Cloning host	Laboratory collection
BL21(DE3)	Overproduction host	Novagen
GM1684	*dam*; for transformation of *B. anthracis*	T. Koehler
Nova blue cells	Cloning host	Novagen
GM2163	*dam*; *dcm* for transformation of *B. anthracis*	New England Biolabs
Plasmids		
E. coli		
pSL1180	Harbors extensive multiple cloning site	Pharmacia
pUCΩKm-2	Harbors Km^r gene flanked by omega elements	62
pES1	Harbors omega Km^r in pSL1180	This study
pET24b	Overexpression vector	Novagen
pMR10	*cotE* overexpression vector	This study
Bifunctional		
pUTE-29	Ap^r in *E. coli*, Tc^r in *B. anthracis*	41
pMR1	Ap^r in *E. coli*, Tc^r and Km^r in *B. anthracis*, with extensive restriction enzyme sites flanking the omega kanamycin resistance gene	This study
pMR4	*cotH* deletion vector	This study
pRG6	*cotB* deletion vector	This study
pRG11	*cotE* deletion vector	This study
pEO-3	*E. coli*/*B. anthracis* shuttle vector	53
pKSM1	pEO-3 + internal fragment of *cotB*	This study
pKSM2	pEO-3 + internal fragment of *cotH*	This study
pKSM3	pEO-3 + internal fragment of *cotE*	This study
pRG23	pEO-3 + internal fragment of *spoIVA* (Sterne)	This study
pEO-3+spoIVA::Ω-Km-2	pEO-3 + *spoIVA*::Km (Ames)	This study

The SacI-SalI fragment of pES1 (bearing ΩKm-2) was ligated into plasmid pUTE29 (41) digested with the same enzymes, resulting in pMR1. To construct each coat protein gene mutation, we used PCR to amplify approximately 1-kb stretches of DNA on either side of each gene using primers. Each resulting pair of DNA fragments was then inserted into pMR1 such that they flanked the kanamycin resistance marker in the plasmid. These recombinant DNA manipulations were carried out using the restriction enzyme sites built into the primers. The plasmids were amplified in *E. coli* GM1684, purified using the QIAGEN Plasmid Mini kit (to increase transformation efficiency) (41), and introduced into the Sterne strain by electroporation. Transformants were selected on the basis of tetracycline resistance as described previously (41).

We isolated recombinants by a two-step procedure. First, we grew transformants in LB medium for 3 days, diluting them by a factor of 1:10 twice a day. On the third day, the culture was plated onto LB agar supplemented with kanamycin. We screened colonies by PCR to confirm that the expected single integration (Campbell-like) event had occurred. To inactivate the target gene, we needed a further reciprocal recombination to excise the plasmid backbone and, in effect, replace the target gene open reading frame with the kanamycin resistance cassette. Therefore, we continued the culture regimen to allow this event to take place. After several days, samples of the liquid culture were plated onto LB agar supplemented with kanamycin. We isolated kanamycin-resistant and tetracycline-sensitive colonies by replica plating and used PCR to confirm that the expected recombination had occurred.

We inactivated *spoIVA* in the Sterne strain by an insertional mutation (53). To do this, we first used PCR and appropriate primers to generate an internal fragment of *spoIVA*. We digested the PCR product and plasmid pEO-3 (53) with BamHI and HindIII and ligated the resulting DNA fragments to build pRG23. We passaged pRG23 through *E. coli* GM1684, introduced it into the Sterne strain by electroporation, and selected for cells in which the plasmid had inserted into the genome by single reciprocal recombination, as described above. This operation inserted the erythromycin-bearing plasmid backbone into *spoIVA* and should generate a null allele, based on extensive analysis of the highly related *B. subtilis* orthologue (11). We then backcrossed this mutation into the Sterne strain by CP51ts-mediated generalized transduction (30). We sporulated the resulting strain (RG154) in the presence of erythromycin, as this was needed to maintain the phenotype (data not shown).

We insertionally inactivated *cotE*, *cotH*, and *cotB* in the Ames strain as previously described (53). To do this, we used PCR (and appropriate primers) to generate DNA fragments corresponding to internal regions of each coat protein gene, digested each fragment with KpnII and NotI, and ligated each fragment with similarly digested pEO-3 (53). We passaged the resulting plasmid through *E. coli* GM2163 cells, introduced it into the Ames strain by electroporation, and selected for integrants as described previously (53).

To insertionally inactivate *spoIVA* in the Ames strain, we first used PCR to generate a DNA fragment bearing the *spoIVA* gene. The fragment was digested with NotI and KpnI and ligated into similarly digested pEO-3 (53). The resulting plasmid was digested with EcoRV (which cuts once within s*poIVA*) and was ligated into a DNA fragment bearing the ΩKm-2 cassette (62), which was generated by SmaI digestion of plasmid pJRS100.2 (M. Caparon, personal communication), a derivative of pJRS102.0 bearing ΩKm-2 at the EcoRI site. This plasmid was then used to transform the Ames strain as previously described (53), and a strain bearing the plasmid as a single reciprocal integration was identified. Next, we cultured this strain in Leighton-Doi medium for several days, as described above for mutagenesis of the Sterne strain, and screened for erythromycin sensitivity and kanamycin resistance to identify a strain (Ames-JAB-11) in which the plasmid backbone had been excised by a reverse reciprocal excision event. We confirmed that this occurred by PCR analysis.

We note that it is highly unlikely that our mutagenesis procedures resulted in significant alterations of the genome beyond what was intended, as in each case, mutations were generated in two backgrounds that produced essentially the same phenotypes (including the case of the *cotB* mutant) (data not shown).

Exosporium isolation and removal. To isolate exosporium material from the Sterne strain, 1×10^9 water-washed spores/ml were passed three times through a French pressure cell at 20,000 lb/in^2. Fragments of the exosporium were then separated from spores by centrifugation at 4,000 × *g* for 15 min. The supernatant was filtered through a 0.45-μm Millex HA filter (Millipore) and was then filtered through a 0.22-μm polyvinylidene difluoride filter (Fisher Scientific) to remove any residual spores. The filtrate was centrifuged at 100,000 × *g* for 1 h, and the resulting pellet was resuspended in 50 mM Tris-HCl and 0.5 M EDTA (pH 8). Pressed spores were washed once with water prior to Western blot analysis. The anti-BclA EG4-4-1 antibody (1.3 mg/ml) was used at a dilution of 1:100,000 to detect exosporium material (78).

Residual exosporium was removed from the Ames strain *cotE* mutant by sonication (5) in a biological safety cabinet, with the spores in a sealed atmosphere chamber and on ice, using a Branson 450 sonifier (Danbury, CT). Spores were then purified by centrifugation through a Hypaque-76 gradient (Nycomed, Inc.) to remove debris. The removal of the exosporium was confirmed by electron microscopy (data not shown).

Antibody production. To produce a polyhistidine-tagged version of CotE in *E. coli*, we used PCR with chromosomal DNA as the template and appropriate primers to generate a DNA fragment encoding CotE. We then digested this DNA fragment with NdeI and XhoI, ligated it with the similarly digested plasmid pET24b (Novagen), and used the resulting plasmid (pMR10) to transform *E. coli* BL21(DE3). We verified that the *cotE* sequence was free of mutations by DNA sequence analysis. We overproduced CotE and purified it from *E. coli* by nickel chromatography according to the manufacturer's directions (Novagen) and contracted with a commercial facility (Sigma Genosys) to produce antibody in rabbits. We used the resulting anti-CotE serum at a dilution of 1:50,000 in Western blot experiments.

Interestingly, neither the *B. anthracis* CotE protein in a spore extract nor *B. anthracis* CotE overproduced in *E. coli* was recognized by a previously generated anti-*B. subtilis* CotE antiserum (data not shown) (4), in spite of the high degree of identity (58%) between these homologues. Likewise, the anti-*B. anthracis* CotE antiserum does not recognize *B. subtilis* CotE (data not shown).

Immunofluorescence microscopy. Ten microliters of culture was placed into each well of a multiwell microscope slide (MP Biomedicals) that was first treated with 0.01% (wt/vol) poly-L-lysine and allowed to dry. The slide was then treated with methanol for 5 min at −20°C and allowed to dry. Ten microliters of phosphate-buffered saline was then placed into each well and was replaced with 2% (wt/vol) bovine serum albumin in phosphate-buffered saline prior to the addition of primary antibody. As primary antibodies, we used either mouse immunoglobulin G1κ1 control antibody (0.5 mg/ml; Pharmingen) at a 1:2,000 dilution or mouse monoclonal anti-BclA EG4-4-1 antibody (1.3 mg/ml) (78) at a 1:5,000 dilution. We used Alexa Fluor 568-conjugated goat anti-mouse antibody (Molecular Probes) as a secondary antibody at a 1:300 dilution. Chromosomes were visualized using the DNA-specific dye Hoechst 33342 (Sigma) (11). Images were collected using a Leica DM IRB fluorescence microscope equipped with a MagnaFire cryocooled charge-coupled-device camera and processed with Adobe Photoshop 7.0 software.

Spore survival in macrophages. RAW264.7 macrophage murine cells (American Type Culture Collection) were infected at a multiplicity of infection of approximately 5 to 10 spores/macrophage and were cultured in Dulbecco's modified Eagle's medium with high glucose, 10% heat-inactivated fetal bovine serum, and 1% sodium pyruvate. Spore survival was measured by in vitro assays, and spores were observed within macrophages by staining as described previously by Welkos et al. (88).

Animal virulence models. (i) Intramuscular challenge experiments. Ten female Hartley Guinea pigs (350 to 400 g each, obtained from Charles River Laboratories) were injected intramuscularly with approximately 2,000 spores of either wild-type or *cotE* or *cotH* mutant strains, representing the equivalent of 20 Ames 50% lethal doses (LD_{50}s) (35). Guinea pigs were monitored several times each day, and mortality rates were recorded.

(ii) Intranasal challenge experiments. Female BALB/c mice (approximately 6 to 8 weeks of age) were anesthetized with 100 μl of ketamine, acepromazine, and xylazine injected intramuscularly. The mice were then challenged with approximately 7.2×10^5 spores of either the wild-type or *cotE* mutant strain, representing the equivalent of 9 Ames LD_{50}s, via intranasal instillation. The total volume of inoculum instilled was 50 μl. Mice were monitored several times each day, and mortality rates were recorded for 14 days.

Statistics. Survival rates were compared between each treatment group and control group by Fisher exact tests with permutation adjustment for multiple comparisons. Mean times to death were compared between each treatment group and control group by *t* tests with permutation adjustment for multiple comparisons. All analyses were conducted using SAS version 8.2 (SAS Institute Inc.).

Identification of gene BAS2377. After SDS-PAGE, a band migrating as a 13-kDa species in a 15% SDS-polyacrylamide gel was excised and digested with trypsin using a MassPrep robot (MicoMass, United Kingdom). The peptides were extracted from the gel plug with 2% acetonitrile–0.1% trifluoroacetic acid and purified and concentrated using C_{18} Zip tips (Millipore). The peptides were eluted from the Zip tips with 5 μl 60% acetonitrile–0.1% trifluoroacetic acid. Two microliters of matrix-assisted laser desorption ionization (MALDI) matrix was added, and the sample was evaporated to dryness in a Speed-Vac, dissolved in ~1 μl of solvent, and spotted in its entirety onto the MALDI target. Mass spectra were acquired using an Applied Biosystems 4700 proteomics analyzer (tandem time of flight). The data from each tandem mass spectrometry spectrum were searched against the NCBI database (accessed in November 2005) using the Mascot search engine (v1.9; MatrixScience, London, United Kingdom).

RESULTS

A survey of coat protein composition in bacilli. Our overall goal was to characterize the coat assembly program in *B. anthracis*. By comparing the *B. anthracis* program with that of *B. subtilis* (Fig. 2), we expected to gain insights into how a basic problem in cellular organization was solved in two related but divergent organisms. This information should identify features of the coat assembly programs that are conserved between species as well as those that vary. As a result, we hope to identify the molecular basis of the taxonomic variation in coat architectures among various species.

We have shown previously that *B. subtilis* and *B. anthracis* have similar numbers of coat proteins, although the electrophoretic patterns differ significantly (44, 46, 68) (Fig. 3, compare lanes 1 and 8). To learn whether this level of polypeptide complexity is a general property of spores of *Bacillus* spp. and therefore to better understand the significance of the differences in the electrophoretic patterns of *B. subtilis* and *B. anthracis*, we examined several other species as well as multiple strains of *B. subtilis* and *Bacillus cereus* (Fig. 3). All the strains that we examined, except for *Bacillus pumilis*, possessed similarly large numbers of coat proteins. Given the morphological differences between the coats of *B. subtilis* and *B. anthracis* as well as the other species (1, 34), we suggest that the degree of structural complexity observed by electron microscopy is not, in general, correlated with the numbers of coat polypeptide

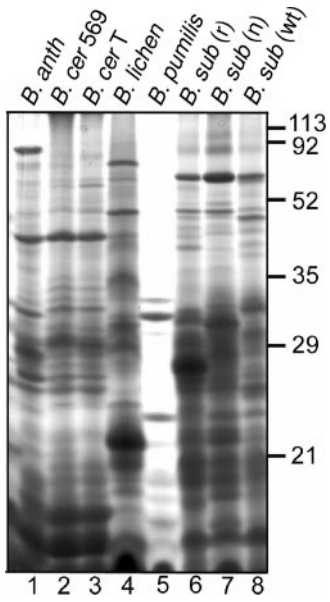

FIG. 3. SDS-PAGE analysis of *Bacillus* spore coat proteins. Spore extracts were fractionated on 15% polyacrylamide gels and stained with Coomassie brilliant blue. Lanes: 1, Sterne strain of *B. anthracis* (RG1) (*B. anth*); 2, *Bacillus cereus* 569 (ADL831) (*B. cer* 569); 3, *B. cereus* T (ADL830) (*B. cer* T); 4, *Bacillus licheniformis* (ADL1392) (*B. lichen*); 5, *Bacillus pumilis* (ADL1391); 6, *B. subtilis* isolated from rabbit (ADL1390) (69) [*B. sub* (r)]; 7, *B. subtilis* natto (ADL1467) [*B. sub* (n)]; 8, *B. subtilis* strain PY79 (ADL18) [*B. sub* (wt)]. Molecular masses are indicated on the right in kDa.

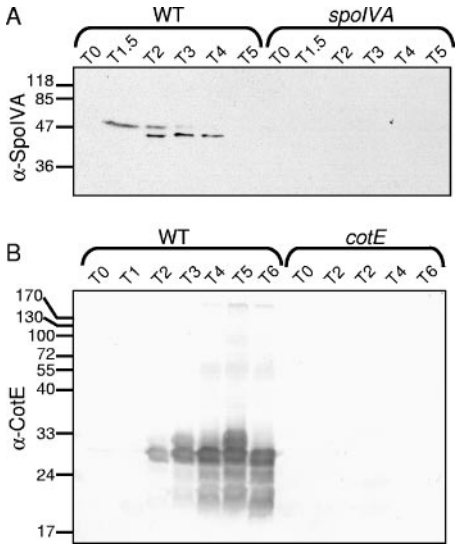

FIG. 4. Western blot analysis of SpoIVA and CotE steady-state levels during sporulation. Sporangial lysates were fractioned by SDS-PAGE and subjected to Western blot analysis using anti-SpoIVA (A) or anti-CotE (B) antibodies. The numbers above the lanes indicate the time in hours after the onset of sporulation, and the genotypes (wild-type Sterne [WT] [strain RG1] or mutant *spoIVA* [strain RG154] or *cotE* [strain RG56]) are indicated above the brackets. Molecular masses are indicated on the left in kDa.

species. For the most part, protein bands from the various isolates did not comigrate, unless they were extracted from spores of strains of the same or closely related species. Therefore, the biochemical composition of coats from different species is likely to vary significantly.

To identify coat protein species shared between *B. subtilis* and *B. anthracis*, we searched their respective genome sequences for orthologues (18, 43, 46, 67). We used recently identified *B. subtilis* coat protein gene candidates (23, 24, 39, 52) and candidates from prior proteomic analyses (44, 46). Of the 86 known *B. subtilis* coat and candidate proteins, at least 65 have homologues in *B. anthracis*, and of these proteins, 25 have paralogues in the *B. anthracis* genome. Thus, *B. anthracis* and *B. subtilis* have similar coat protein repertoires and share almost all of the known morphogenetic proteins (18).

Role of SpoIVA in *B. anthracis*. Given the importance of the morphogenetic coat proteins SpoIVA, CotE, and CotH in *B. subtilis* (19), we analyzed the phenotypes of *B. anthracis* strains (both Sterne and Ames) bearing mutations in the corresponding homologues. The resulting strains grew normally and entered sporulation, as judged by light microscopy (data not shown). However, the *spoIVA* mutant strains in the Sterne and Ames backgrounds (RG154 and JAB11, respectively) both failed to progress beyond very early stages of sporulation. Light microscopy revealed that neither strain developed refractile forespores during sporulation or released a refractile body after extended culturing under sporulation conditions (data not shown).

To precisely determine the nature of the sporulation defect in these cells, we carried out thin-section electron microscopy. We found that after a period of sporulation that was sufficient to allow the formation of mature forespores in sporulating cells of a wild-type strain, *spoIVA* mutant sporulating cells were clearly defective (Fig. 1C and D and data not shown). The forespores lacked the germ cell wall or cortex, and the mother cells were filled with swirls of electron-dense material (Fig. 1D and data not shown). This is extremely close to the *B. subtilis spoIVA* mutant phenotype, where we know that the swirls are unattached coat material (20, 70). Based on the lack of forespore-associated structures, the swirls of material in the mother cell, and the *B. subtilis spoIVA* mutant phenotype, we consider it very likely that these swirls contain both coat and exosporium material. We infer, therefore, that as in the case of *B. subtilis*, SpoIVA is responsible for the attachment of the coat (and, indirectly, the exosporium) to the forespore surface (20, 64, 65).

The view that SpoIVA in *B. anthracis* directs early sporulation events, such as the initial assembly of the coat and cortex, requires that the protein be synthesized at an appropriately early time. To test this, we carried out Western blot analysis using anti-*B. subtilis* SpoIVA antibodies (11). We detected 47-kDa and 45-kDa species in sporulating cells of the Sterne strain (but not the *spoIVA* mutant) beginning at 1½ h after the onset of sporulation (Fig. 4A), consistent with the timing of *spoIVA* gene expression from microarray analysis (for *B. anthracis*) (50) and Northern blot analysis (for *B. subtilis*) (70). The 47-kDa species was not detected after hour 3. Neither species was detectable after hour 4, likely as a result of the difficulty of extracting the protein when the maturation of the coat proceeded past an intermediate stage. Taken as a whole, we interpret these experiments to indicate that in *B. anthracis*, as in *B. subtilis*,

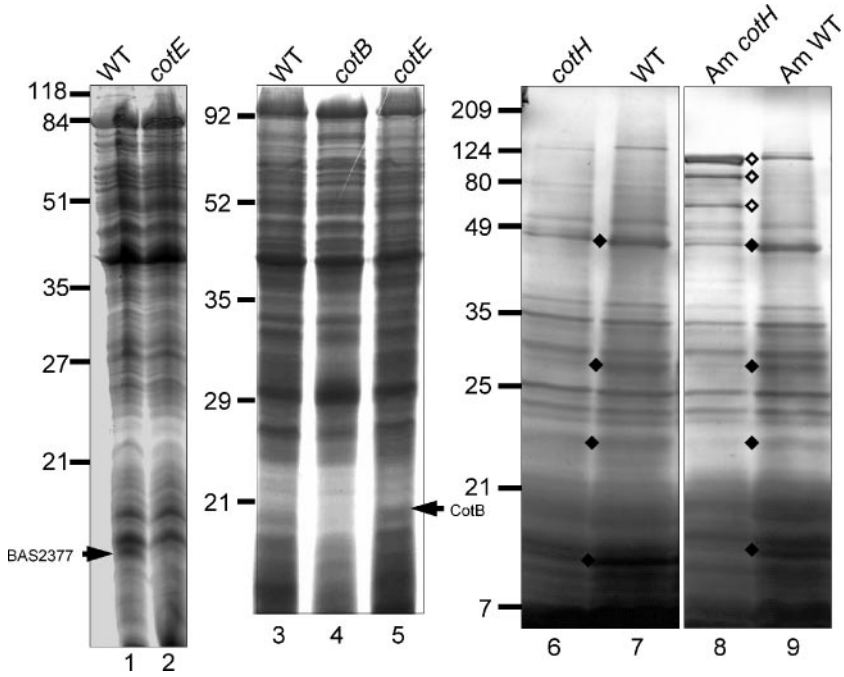

FIG. 5. SDS-PAGE analysis of spore coat proteins from wild-type (WT) and mutant *B. anthracis*. Proteins were extracted from spores harvested after sporulation in Difco sporulation medium (in lanes 1 to 5) or Leighton-Doi medium (in lanes 6 to 9). Proteins were fractionated on 15% (lanes 1 to 5) or 16% (lanes 6 to 9) polyacrylamide gels and stained with Coomassie brilliant blue. The figure shows electrophoretic profiles of extracts from Sterne wild-type (strain RG1) (lanes 1, 3, and 7) and *cotE* (strain RG56) (lanes 2 and 5), *cotB* (strain RG35) (lane 4), and *cotH* (strain RG73) (lane 6) mutant strains or Ames *cotH* mutant (strain JAB3) (lane 8) and wild-type (lane 9) strains. Arrowheads indicate the positions of CotB and the putative CotE-controlled protein BAS2377; open diamonds indicate 116-, 92-, and 70-kDa bands whose intensities increase in the JAB3 extract; and closed diamonds indicate 43-, 29-, 24-, and 13-kDa bands whose intensities decrease in strains RG73 and JAB3. Molecular masses are indicated in kDa.

SpoIVA is required for germ cell wall and cortex formation and for attachment of the coat.

Role of CotE in *B. anthracis*. Sterne and Ames *cotE* mutant strains (RG56 and JAB4, respectively) grew and sporulated normally, as does the corresponding *B. subtilis* mutant (94). Strikingly, however, thin-section electron microscopy revealed that the majority of *cotE* mutant spores had significantly impaired assembly of the exosporium (in strains RG56 and JAB4) (Fig. 1E to H). The coat, which is a thin, compact structure, is evident on the outer surface of the cortex (or separated from it, as discussed below). The exosporium, which is morphologically distinct (and, in particular, is distinguished by its hair-like projections), in these cases, is either present as fragments (data not shown) or missing entirely (Fig. 1E to H). Therefore, CotE is required for the normal appearance of the exosporium around the spore. Although present, the coats in the *cotE* mutant spores were not entirely normal in that they were often partially or fully detached from the underlying spore peptidoglycan. The surfaces of these detached coats were smooth, lacking the folds that typically appear as the spore core shrinks during sporulation (Fig. 1, compare A and B to E and H). This is very similar to the *B. subtilis cotE* phenotype in which the coat similarly detaches from the spore peptidoglycan (16, 94). Presumably, surface ridges unfold because of the lack of a connection with the underlying cortex (17).

To more carefully characterize the *cotE* spore surface, we imaged it in the dry state by AFM in the tapping mode, a method that generates a topographical relief map (25, 76). Wild-type Sterne strain spores have ridges on the coat surface that extend in a relatively straight line from pole to pole (12) (Fig. 1I). In contrast, the *cotE* Sterne strain mutant had either a series of disorganized ridge-like structures that usually did not span the long axis of the spore (Fig. 1J) or no ridges at all (Fig. 1K). In the latter case, the mutant spore coat surfaces resembled those of the corresponding *B. subtilis* mutant (12).

By using thin-section electron microscopy, we detected inner and outer layers in Sterne *cotE* mutant spores (Fig. 1F, inset), in contrast to the corresponding *B. subtilis* mutant, which lacks an outer coat (94). To characterize the composition of the *cotE* mutant spore coat, we visualized the extractible coat proteins after fractionation by SDS-PAGE. In *B. subtilis*, a *cotE* mutation results in the loss of about half of the bands that are normally present (4, 48, 94). In contrast, the electrophoretic patterns of extracts of wild-type and *cotE* Sterne spores were very similar (Fig. 5, lanes 1 and 2, respectively). The major consistent difference between wild-type and mutant spore extracts was the absence of a band migrating as an approximately 13-kDa species. In *B. subtilis*, especially severe changes in coat composition, including those due to the *cotE* mutation, can impair the ability of the coat to function as a sieve that excludes large molecules, as measured by the ability to exclude lysozyme (1, 4, 14). To determine whether this is the case for the *B. anthracis cotE* mutant, we incubated spores form strain RG56 with lysozyme. We found that these spores were not detectably more sensitive to lysozyme than the wild type, consistent with

the view that the coat is not severely disrupted by the mutation. Therefore, in *B. anthracis*, CotE has a major role in exosporium assembly but a more limited, although significant, role in coat formation.

To identify the CotE-dependent 13-kDa band (Fig. 5, lane 1), we harvested it from a polyacrylamide gel and performed MALDI–time-of-flight mass spectrometry. This analysis identified a protein encoded by an open reading frame in the Sterne strain, currently designated BAS2377, whose predicted molecular mass is 12 kDa. This protein does not resemble other proteins in the databases, except the ones encoded in the genomes of the closely related species *B. cereus*, *Bacillus weihenstephanensis*, and *Bacillus thuringiensis*. We therefore tentatively suggest that this protein is a component of the spore specific to the so-called *B. cereus* group of species. We have not yet named this gene because we do not know if this protein is located in the coat, exosporium, or interspace. Interestingly, CotH may also control BAS2377 assembly (see below).

In *B. subtilis*, CotE controls the assembly of at least 24 coat proteins (39, 48, 94). Sixteen of these proteins have orthologues in *B. anthracis*, and for eight of them, paralogues are present as well. Given the modest role of CotE in *B. anthracis* coat protein assembly (Fig. 5, lane 2), it appears that CotE is required for the assembly of very few, if any, of these orthologues and paralogues. To investigate this finding further, we tested whether CotE has a role in the assembly of the two *B. anthracis* orthologues of CotB (46), as the assembly of *B. subtilis* CotB is known to be CotE controlled (39, 52, 94). First, we generated a version of the Sterne strain (RG35) in which the *cotB* orthologues were deleted. As anticipated, a band previously identified as a CotB orthologue was undetectable in spore extracts from the *cotB* mutant (Fig. 5, lane 4) but was present in *cotE* mutant spores (Fig. 5, lane 5), suggesting that *B. anthracis* CotB is CotE independent.

In *B. subtilis*, CotE is synthesized early in sporulation, consistent with its role at an early stage in coat assembly (94). The mutant phenotypes for strain RG56 left unclear whether CotE acts early or late in the sporulation in *B. anthracis*. To help clarify this, we monitored the steady-state levels of CotE over the course of sporulation by using Western blot analysis with an anti-CotE antiserum. We first detected CotE 2 h after the start of sporulation (Fig. 4B). At all time points, we detected a prominent band migrating as a 26-kDa species, which is likely to be the monomer. At later times, we detected slower-migrating species, including bands at 55 kDa and a band that migrates as larger than 170 kDa, which are likely the result of cross-linking. In addition, we detected smaller species between 17 and 26 kDa, which are probably due to proteolysis. Similar low-molecular-weight bands were detected previously in similar experiments with *B. subtilis* (4). The effect of CotE on both coat and exosporium assembly (Fig. 1) is consistent with a possible location in either or both structures. To address this, we separated the exosporium from Sterne strain spores using a French press and differential centrifugation and analyzed both fractions by Western blot analysis using anti-*B. anthracis* CotE and anti-BclA antibodies to identify coat and exosporium material, respectively (Fig. 6A and B). The CotE antiserum specifically recognized multiple species at less than 26 kDa (Fig. 6A). Differences between the bands of sporangial or spore extracts detected in Western blot analysis raise the possibility

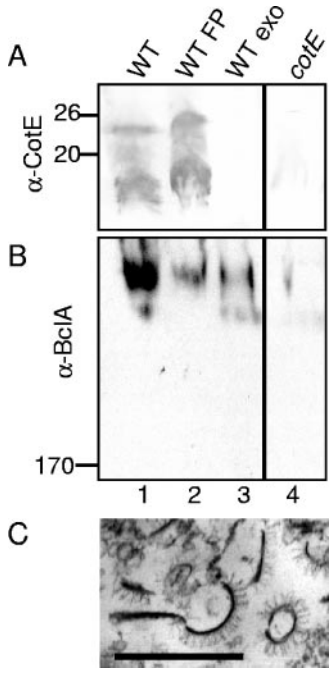

FIG. 6. Subcellular localization of CotE in Sterne strain spores. Spore proteins from wild-type (WT) (strain RG1) (lanes 1 to 3) or *cotE* mutant (strain RG56) (lane 4) spores were fractionated by SDS-PAGE and subjected to Western blot analysis using anti-CotE (A) or anti-BclA (B) antibodies. Lanes: 1, intact wild-type spores; 2, French-pressed wild-type spores; 3, wild-type exosporium fraction; 4, intact *cotE* spores. Molecular masses in kDa are indicated on the left. Thin-section electron microscopy was used to verify the purity of the exosporium fraction (C). The size bar indicates 500 nm.

of modifications of CotE during coat assembly. The anti-BclA antibody recognized a species larger than 170 kDa in the Western blot analysis of spore extracts, consistent with previous reports (Fig. 6B, lane 1) (78, 80, 81). Even after French press treatment, at least some exosporium was still spore associated, as judged by Western blot analysis (Fig. 6B, lane 2). More importantly, CotE was undetectable in the exosporium fraction (Fig. 6A, lane 3). As expected, we did not detect bands with either antibody when we analyzed extracts of the *cotE* mutant (Fig. 6A and B, lane 4). The exosporium fraction was free of spores, as judged by light and electron microscopy (Fig. 6C and data not shown). Therefore, CotE is largely, if not entirely, restricted to the coat or the interspace. Given that CotE is a coat protein in *B. subtilis* (20, 94), our working model is that CotE is also a coat protein in *B. anthracis*.

If CotE is not in the exosporium, then its role in exosporium assembly is likely to be solely in the attachment to the spore and not in exosporium synthesis. To investigate this further, we used thin-section electron microscopy of sporulating Sterne strain cells over an 8-h period to document exosporium formation and to pinpoint the role of CotE in the process. We first detected a structure, possibly related to the exosporium, in cells that appeared to be about to complete, or to have just completed, forespore engulfment (Fig. 7A). In a low percentage (<5%) of these cells, we observed a thin electron-dense layer adjacent to the forespore on the mother-cell-proximal surface. The lengths of these layers varied, but we never found

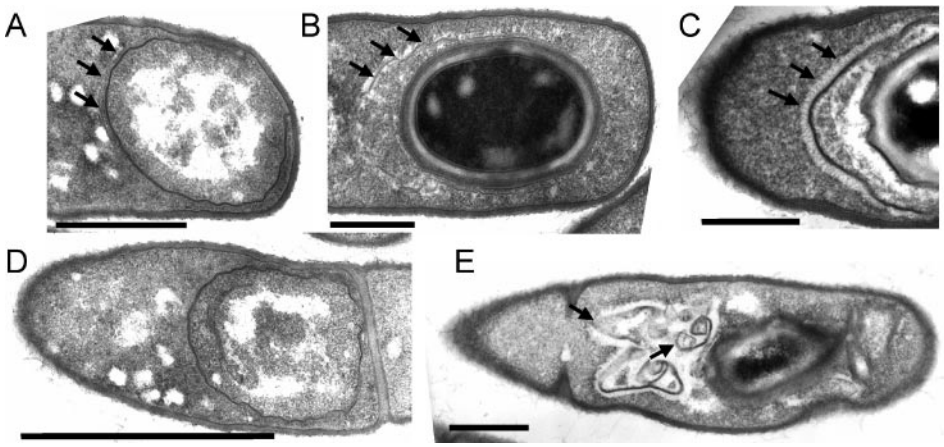

FIG. 7. Thin-section electron microscopic analysis of exosporium assembly in the Sterne strain. Wild-type (RG1) (A to C) and *cotE* mutant (RG56) (D and E) cells at hours 2 (A and D), 4 (B), and 8 (C and E) were analyzed. The arrows indicate layers of material that we interpret as exosporium or early exosporium material. Bars indicate 500 nm.

a case where the forespore was fully encircled at this early time. In cells that had progressed to the point of at least partial cortex formation, the forespore-associated layer-like material was significantly more electron dense in a significant percentage of cells (Fig. 7B). In cells that had advanced further in development, as evidenced by the deposition of at least some coat material and/or spore core dehydration, the layers clearly had the characteristics of a mature exosporium (Fig. 7C). These observations are essentially the same as those described previously for *B. cereus* exosporium formation (59). In *cotE* sporangia, we did not detect layer-like structures adjacent to the forespore at an early time in sporulation, even after exhaustive analysis (Fig. 7D and data not shown). However, we observed the accumulation of exosporium-like material in the mother cell cytoplasm (Fig. 7E).

To confirm that the swirls visualized in the *cotE* mutant sporangia by electron microscopy are exosporium, we carried out immunofluorescence microscopy using anti-BclA antibodies (Fig. 8) and isotype-matched antibodies as a negative control (data not shown). Application of the DNA-binding stain Hoechst 33342 allows the visualization of the mother cell chromosome but not the forespore chromosome, as the stain is excluded from the forespore at this time point (hour 8). Wild-type cells showed a ring of anti-BclA fluorescence that we inferred to be around the forespore based on the position of the mother cell chromosome (Fig. 8A). In contrast, in about 90% of cases, *cotE* mutant cells possessed a region of fluorescence in the mother cell cytoplasm (Fig. 8B). In the remaining 10% of cases, we detected rings or partial rings of fluorescence around the forespore (data not shown). The isotype control experiment showed no cross-reactivity in either strain (data not shown). Taken together, we interpret these results to indicate that the *cotE* mutation does not detectably affect exosporium synthesis but rather prevents its attachment to the forespore. If CotE is a coat protein, it may participate in connecting the exosporium to the coat surface (see Discussion).

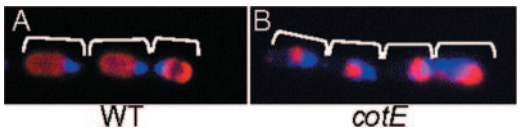

FIG. 8. Immunofluorescence microscopic detection of BclA. Sporangia from strain RG1 (wild type [WT]) (A) and strain RG56 (*cotE* mutant) (B) were harvested at hour 8 of sporulation, fixed, and treated with the anti-BclA EG4-4-1 monoclonal antibody (red). Mother cell chromosomes were stained with Hoechst 33342 dye (blue), which is excluded from the forespores at this point in development. The locations of individual cells (indicated by brackets) were determined based on bright-field microscopy (data not shown).

In the course of this analysis, we observed that in wild-type cells with mature but unreleased spores, the interspace width was not constant around the spore circumference (data not shown). Specifically, it appeared that the interspace width was smaller where the spore was closest to the mother cell envelope (i.e., along the short axis of the oval spore) and larger where there was no restriction (i.e., along the long axis of the spore). We interpret this, as well as the increase in interspace width upon spore release, to be evidence that the interspace is compressible and has a spring-like nature (see Discussion). However, the irregularity of the interspace width along the circumference of a released spore indicates that this spring-like property is probably not uniform throughout the interspace.

In *B. subtilis*, coat proteins with significant roles in coat assembly usually also affect germination (16). In *B. anthracis*, conversion of the spore to the vegetative state is essential for infection (54). Therefore, we studied the possible involvement of *B. anthracis* CotE in germination (55, 74). To measure early events in germination, we used a calcium release assay (87) for the Sterne strain and a quantitative fluorescent dye uptake assay for both the Sterne and Ames strains (89) (since safety considerations make the use of radioactivity, needed for the calcium release assay, inappropriate for use with Ames). *cotE* mutant spores from the Sterne and Ames strains had significant delays in early germination events based on the dye uptake assay and significant, although much more modest, delays based on the calcium release assay (Fig. 9A and C). Differences in the sporulation media used in the two assays prevent direct comparisons of the data generated using different meth-

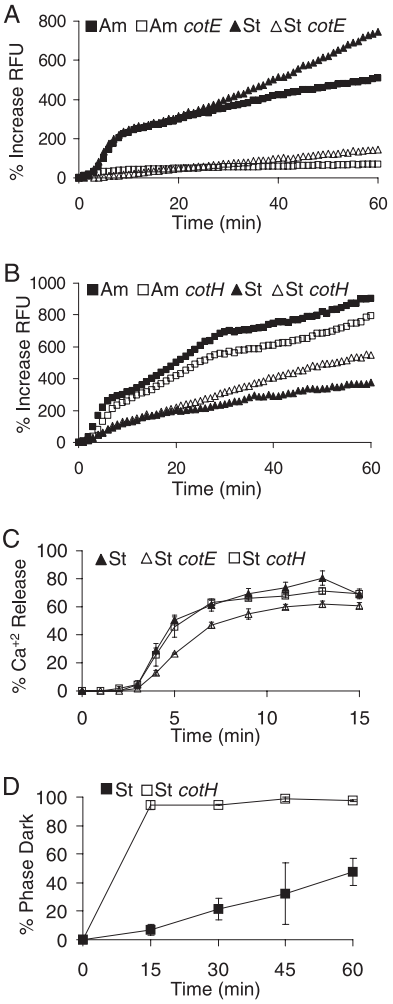

FIG. 9. Effects of coat protein gene mutations on germination. Fluorescent dye uptake (A and B) and calcium release (C) assays and phase-contrast microscopy (D) were used to measure germination. All assays were done in triplicate, and standard errors of the means are indicated for panels C and D. Representative data are shown for panels A and B. The percent increase in the relative fluorescent unit (RFU) value of a sample is the difference between the RFU at a given time in germination medium and the RFU at time zero, expressed as a percentage of the latter. The percentage of phase-dark spores was calculated as follows: (total number of spores − number of phase-bright spores)/total number of spores. Am, Am *cotE*, Am *cotH*, St, St *cotE*, and St *cotH* indicate Ames wild type, Ames *cotE* mutant (JAB4), Ames *cotH* mutant (JAB3), Sterne wild type (RG1), Sterne *cotE* mutant (RG56), and Sterne *cotH* mutant (RG73), respectively.

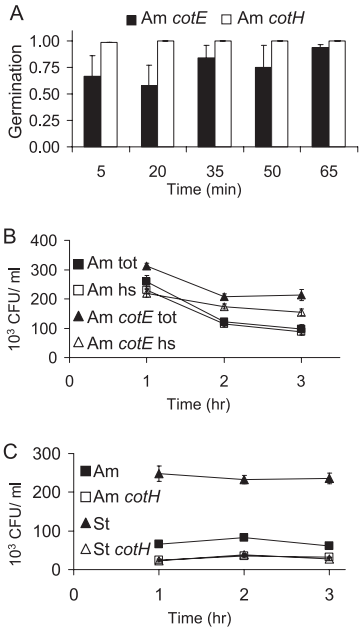

FIG. 10. Effects of coat protein gene mutations on germination and spore survival in macrophages. Spores were suspended in BHI medium, and the percentage of heat-sensitive *cotE* or *cotH* mutant or wild-type cells was determined at each time point. Percent germination of the mutant cells was normalized to that of the wild type. Therefore, a ratio of 1 indicates wild-type levels of germination, and a value less than 1 indicates a germination defect (A). Spore survival in macrophages was measured by CFU determinations with or without heat shocking (B and C). All assays were done in triplicate, and standard errors of the means are shown. Am, Am *cotE*, Am tot, Am hs, Am *cotE* tot, Am *cotE* hs, Am *cotH*, St, and St *cotH* indicate Ames wild type, Ames *cotE* mutant (JAB4), Ames wild-type total, Ames wild type after heat shock, Ames *cotE* mutant (JAB4) total, Ames *cotE* mutant (JAB4) after heat shock, Ames *cotH* mutant (JAB3), Sterne wild type (RG1), and Sterne *cotH* mutant (RG73), respectively.

ods. To measure later germination events, we monitored the appearance of heat-sensitive (i.e., germinated) spores after resuspension in BHI medium. Even though it begins to appear early in germination, heat sensitivity can be an appropriate measure for later events, as the acquisition of complete heat sensitivity occurs relatively late (56, 74). *cotE* spores were partially germination defective, as measured by the loss of heat resistance during incubation in BHI medium (Fig. 10A and data not shown).

To monitor the completion of germination, we measured the ability of spores to resume metabolism after germination by using a variant of the semiquantitative tetrazolium overlay assay, which is well established in studies of *B. subtilis* (14). This assay produces a color reaction whose intensity is a measure of the resumption of metabolism. We were able to detect a slight reduction in the color intensity produced by the *cotE* mutant strain (RG56) compared to that produced by the wild type (data not shown), suggesting a defect in the completion of germination, consistent with the results of the heat sensitivity assay.

Germination in phagocytic cells is very likely to be important to anthrax pathophysiology (15, 31). We have argued previously that when spores germinate, they become sensitive to macrophage killing (88). Therefore, we addressed the question of whether the in vitro germination defect of *cotE* mutant spores (discussed above) affected germination in macrophages. After macrophage infection, we recovered more *cotE* mutant cells than wild type Ames cells, as would be anticipated for germination-defective spores (Fig. 10B). To further address whether the increase in the number of *cotE* mutant cells recovered from macrophages was due to a germination defect, we harvested bacteria from spore-infected macrophage cultures and measured germination by testing heat sensitivity. Surprisingly, we found that *cotE* spores survive in the macrophage even after losing heat resistance (i.e., after germination),

as the total number of Ames strain cells recovered from the macrophage was greater than the number of heat-resistant (ungerminated) cells (Fig. 10B). This was true for the Sterne strain *cotE* mutant as well (data not shown). In contrast, and as expected, after infection by the wild-type Ames strain, the number of heat-resistant bacteria (i.e., ungerminated spores) was similar to the total number of cells recovered (Fig. 10B). Therefore, the germination defect in *cotE* mutant spores cannot fully explain their ability to survive in the macrophage. One possible explanation for the survival of these spores would be an inherent heat resistance defect of dormant *cotE* mutant spores (as opposed to a defect in germination per se). If this were true, heat resistance would not accurately reflect germination, since the dormant spores would be heat sensitive. We ruled out this possibility, however, as dormant *cotE* mutant spores do not have a heat resistance defect (data not shown). Given this, it is not immediately obvious how to account for our data, since we would expect heat-sensitive cells to have also shed the coat, making them vulnerable to macrophage lysozyme. We favor the possibility that coat shedding is delayed in *cotE* mutant spores, thereby allowing them to endure macrophage stress even after a loss of heat resistance.

We also detected a defect in *cotE* mutant spore germination in macrophages by using a stain that distinguishes dormant and germinating spores (91; data not shown). In the case of infection with wild-type Ames, after 1 h of incubation, most spores within macrophages were committed to germination, as indicated by a purple counterstain. In contrast, when macrophages were infected with *cotE* mutant spores, the majority of spores in macrophages stained with malachite green, indicating that germination had not initiated (data not shown). After 2 h of additional incubation, 62% of the intracellular *cotE* mutant spores were counterstained purple, compared to 99% of the intracellular wild-type (Ames) spores, consistent with the results described above (data not shown). Taken as a whole, these data indicate that both Sterne and Ames strain *cotE* mutants have a partial defect at an early stage in germination and, possibly, at a later stage. This could be due to changes in the coat, exosporium, or both.

Role of CotE in virulence. Previously, it was shown that the major exosporium protein BclA is dispensable for infection by the attenuated Sterne strain in an immunocompromised mouse model (80). The exosporium defect of *cotE* mutant spores allowed us to evaluate the role of all the exosporium components in disease by using a virulent strain. We sonicated *cotE* mutant Ames strain spores to completely remove any residual exosporium and tested their ability to cause infection in a Guinea pig intramuscular challenge model (35). Spores that were missing their exosporia were fully virulent in this model (Fig. 11A). Furthermore, taken together with the data described above, we conclude that modest defects in germination do not necessarily prevent disease.

Although our results indicate that the exosporium is not essential for causing infection, the inhalational form of the disease may depend on the exosporium. For example, exosporia could aid the passage of the spore through the respiratory epithelium or somehow facilitate dissemination by phagocytic cells that presumably move spores from the lung to the mediastinum. Therefore, we tested the ability of sonicated *cotE* spores lacking exosporia to cause disease in a mouse intranasal challenge model (51). As with intramuscular challenge, exosporium-deficient *cotE* spores were fully virulent (Fig. 11B). In this model, we did not observe any significant differences in survival rates ($P > 0.9999$) or in the mean times to death ($P = 0.1809$) between challenges with Ames or *cotE* spores.

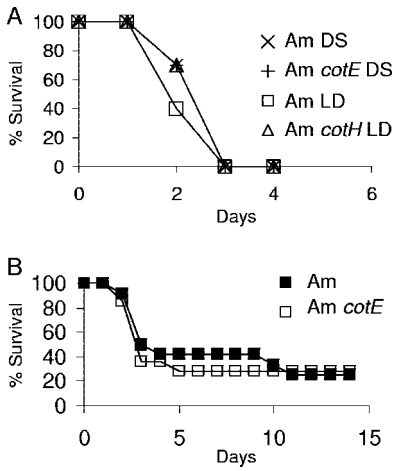

FIG. 11. Analysis of wild-type and mutant spores in Guinea pig intramuscular and mouse intranasal challenge assays. Wild-type or mutant spores were used in Guinea pig intramuscular (A) or murine intranasal (B) challenge experiments, and survival was recorded. Am DS, Am *cotE* DS, Am LD, Am *cotH* LD, Am, and Am *cotE* indicate Ames wild-type cells cultured on Difco sporulation agar, *cotE* Ames mutant (JAB4) cells cultured on Difco sporulation agar, Ames wild-type cells cultured in Leighton-Doi medium, *cotH* Ames mutant (JAB3) cells cultured in Leighton-Doi medium, Ames wild-type spores, and sonicated *cotE* mutant (JAB4) spores, respectively.

Role of CotH in *B. anthracis*. In *B. subtilis*, the CotE-controlled protein CotH directs the assembly of at least seven coat proteins (39, 48, 57; M. Hahn and A. Driks, unpublished observations). The *B. anthracis* CotH homologue is 56% identical and 72% similar to the *B. subtilis* protein. We tested the role of CotH in *B. anthracis* spore function and assembly by inactivating its gene in the Sterne and Ames strains (resulting in strains RG73 and JAB3, respectively) and analyzing the resulting cells as we did for the *cotE* mutant. *cotH* mutant cells grew and sporulated normally and were indistinguishable from the wild type by light and thin-section transmission electron microscopy (data not shown). However, AFM analysis of the Sterne *cotH* mutant strain revealed that the coat surface ridges were largely absent (Fig. 1L). SDS-PAGE analysis revealed differences in the electrophoretic patterns of Coomassie-stainable bands from extracts of wild-type and *cotH* mutant spores in both the Sterne and Ames backgrounds (Fig. 5, lanes 6 to 9). In particular, bands of 43, 29, 24, and 13 kDa were reduced in intensity in mutant strain extracts. The 13-kDa band may be BAS2377, which is controlled by CotE (see above). In most analyses, we also detected increased amounts of the 116-, 92-, and 70-kDa bands in the Ames mutant. Because the changes in the *cotH* electropherogram were more severe than those seen for the *cotE* mutant, it is unlikely that CotH is a CotE-controlled protein in *B. anthracis*, as it is in *B. subtilis* (95).

We analyzed the ability of the *cotH* mutants to germinate, as described above. In contrast to the case of *cotE*, *cotH* mutants of either the Sterne or Ames background showed no significant

defect by calcium release, dye uptake, or heat resistance (when germinated in BHI medium) (Fig. 9B and C and 10A and data not shown). However, we were able to detect differences in the *cotH* mutant strains in the following assays. First, we measured the ability of spores to resume metabolism after germination by using a modified tetrazolium assay (described above). *cotH* mutant strains (RG73 and JAB3) produced a color that was greater in intensity than that produced by the wild type (data not shown). This could occur if the percentage of *cotH* mutant spores that successfully germinate is higher than that of wild-type spores. Therefore, we germinated wild-type and *cotH* mutant cells (RG1 and RG73) (in triplicate) and monitored the refractility of spores by phase-contrast light microscopy (Fig. 9D). At the initiation of germination, all of the spores were phase bright, indicating a dehydrated, and therefore dormant, spore. After 15 min of germination, 7% of wild-type spores had become phase dark, and 94% of *cotH* mutant spores were phase dark, consistent with the results of the tetrazolium overlay assay and indicating that more *cotH* mutants spores germinated than wild-type spores. After 60 min, 47% of wild-type spores were phase dark, while 98% of the *cotH* mutant spores had become phase dark. We also examined the role of CotH in germination by assessing spore survival after uptake by macrophages. We found that fewer *cotH* mutant spores were recovered after macrophage uptake, consistent with an increase in *cotH* mutant spore germination (Fig. 10C). Overall, our measurements of early and intermediate events in germination by calcium release, dye uptake, or heat resistance suggest that these occur largely normally in *cotH* mutants, whereas the other assays, phase-dark transition and macrophage survival, indicate that more *cotH* mutant spores complete germination than do wild-type spores. Because we used the same germinant to detect the consequence of the *cotH* mutation when calcium release was analyzed, dye uptake and phase transition, our data suggest a defect in a relatively late stage in germination that results in an increase in the number of germinating spores. Regardless, the *cotH* mutation does not appear to have a dramatic effect on disease, as the *cotH* mutation had no effect on virulence in the Guinea pig intramuscular challenge virulence model (Fig. 11A).

DISCUSSION

There are two major conclusions from this study. First, we characterized the phenotypes of *B. anthracis* strains bearing mutations in *spoIVA*, *cotE*, and *cotH*, homologues of important *B. subtilis* coat protein genes. Our data allow us to construct a preliminary model for coat and exosporium assembly in *B. anthracis* (Fig. 2E to H). Comparison of this model with the *B. subtilis* model reveals that while the core morphogenetic proteins are conserved between these species, the actions of some of these core factors differ significantly. The second major result from this work is the discovery that the exosporium is dispensable for the establishment of infection in both intramuscular challenge and intranasal models of infection, at least in the context of a *cotE* mutant.

A model for assembly in *B. anthracis*. The results presented here allow us to describe the outlines of coat assembly in *B. anthracis* (Fig. 2E to H). In this view, the first critical event in *B. anthracis* coat assembly is the deposition of SpoIVA at the forespore surface (as is also the case in *B. subtilis*) (Fig. 2A and E). We expect this to be true in *Clostridium* spp. as well, since extremely close homologues of *spoIVA* are present in the genomes of the sequenced strains from this genus. Next, a shell of CotE forms (or begins to form) around the spore (Fig. 2F) in a SpoIVA-dependent manner, as in *B. subtilis*. CotE, in turn, directs the assembly of an electron-translucent structure that assembles at the mother cell pole of the forespore. The surface of this structure could serve as the site of exosporium assembly initiation. This early coat structure is reminiscent of the precoat in *B. subtilis* (20). Once coat and exosporium assembly begin, their formation proceeds essentially concomitantly, with the layers of the coat becoming evident, the exosporium forming a contiguous shell, and the eventual appearance of the hair-like projections (Fig. 2G). Soon after forespore engulfment, the close connection between the "precoat" and the exosporium apparently changes, resulting in variability in the size of the interspace around the circumference of the spore. We speculate that the spring-like quality of the interspace mentioned above appears at this time. The exosporium has previously been observed to be flexible in *Bacillus mycoides* (6), perhaps due to the spring-like nature of the interspace. We also infer that an as-yet-unidentified material spans the interspace to connect the coat and exosporium and that CotE attaches this material to the coat (Fig. 2H). Although no connecting material is evident by thin-section electron microscopy, we assume that it exists, as otherwise, the exosporium would not close around the spore during its assembly.

How CotE guides the exosporium around the forespore is unclear. Possible clues are provided by recent results showing that the spore proteins ExsY and CotY play important roles in exosporium assembly in *B. anthracis* and in *B. anthracis* and *B. cereus*, respectively (7, 37). Interestingly, ExsY and CotY are orthologues of the *B. subtilis* CotE-controlled protein CotZ (39). This raises the speculative possibility that CotE directs exosporium assembly at least partially through the control of ExsY and CotY. Notably, in *B. anthracis exsY* mutant sporangia, a fragment of exosporium is detected at the mother-cell-facing pole of the forespore (7). This suggests that the *cotE* mutant phenotype is more severe than that of *exsY*, consistent with the speculations mentioned above.

CotH plays a significant role in the deposition of certain coat proteins in both *B. anthracis* and *B. subtilis*. The observation that germination appears to be increased in the *B. anthracis cotH* mutant spores raises the possibility that CotH controls the assembly of germination-inhibitory proteins. We do not know how CotH assembly is controlled. However, the phenotypes of *cotE* and *cotH* mutants indicate that CotE and CotH assemble largely independently. The previously identified *B. anthracis* morphogenetic coat protein, Cotα, is also likely to assemble independently of CotE or CotH, given that the *cotα* mutant coat assembly phenotype is more severe than that of a *cotE* or *cotH* mutant (40). However, phenotypic comparisons do not exclude the possibility that Cotα directs CotH assembly.

The phenotypic differences between *cotE* and *cotH* mutants in *B. anthracis* and *B. subtilis* are reminiscent of the differences in the morphological consequences in mutations in *safA* in *B. subtilis* and its orthologue, *exsA*, in *B. cereus* (3). ExsA, which controls coat and exosporium assembly in *B. cereus*, appears to

have a more severe effect on the *B. cereus* coat than does *safA* on the *B. subtilis* coat (60, 82).

By approximately hour 8 of sporulation, the exosporium has divided the mother cell into two compartments. Given that the exosporium is probably impermeable to proteins (27, 29, 42), it is reasonable to suggest that after hour 8, any assembly at the coat or the underside of the exosporium depends on proteins in the interspace. It might be argued that the number of ribosomes in this region is insufficient to synthesize sufficient amounts of coat proteins. However, we have proposed that coat proteins are synthesized in excess in *B. subtilis* (11). Possibly, a similar excess of coat proteins in *B. anthracis* facilitates continued assembly after closure of the exosporium.

CotE has a poorly characterized common role in both *B. subtilis* and *B. anthracis*: enforcing close contact between the coat and the cortex (4, 16). Possibly, CotE imparts an elastic property to the coat. In this view, as the forespore volume decreases (during core dehydration), the coat maintains contact by constricting in a CotE-dependent manner. In the absence of CotE, this elastic property is lost and the coat retains the larger diameter that it possessed prior to forespore dehydration. This perspective implies that the contacts that mediate the initial deposition of CotE at the forespore are of low affinity or otherwise lost as development proceeds. The elasticity could be a direct result of CotE or CotE-controlled proteins, or it could be an emergent property of the entire coat. An additional common role for CotE in *B. subtilis* and *B. anthracis* is in germination (94). It seems likely that the mechanistic basis of the impact of CotE on germination will differ between these species due to the different roles in coat assembly. However, in *B. subtilis*, CotE controls the assembly of CwlJ, which participates in a redundant pathway in later stages of germination (2, 61) and has two homologues in *B. anthracis*, as identified by BLAST analysis. Possibly, in *B. anthracis*, CotE controls CwlJ assembly as well.

Our data are consistent with the view that various *Bacillus* species use a conserved core of morphogenetic coat proteins in related but different ways. This raises the possibility that relatively modest numbers of mutations in the morphogenetic coat protein genes would permit significant changes in function and enable rapid adaptation to novel niches. This would be particularly useful to bacilli, given the diversity of environments that they inhabit (58, 66). From analyses of coat protein gene sequences of a variety of species, it may be possible to address this issue by measuring the degree of evolutionary pressure on key amino acids of morphogenetic coat proteins.

The exosporium is probably not a virulence factor. A principal result from this work is the finding that, at least in the context of a *cotE* mutation, the exosporium is dispensable for virulence as measured in two animal models. As the outermost surface of the *B. anthracis* spore, it is reasonable to imagine that the exosporium plays a significant role in disease. However, Sylvestre et al. (80) showed that a deletion of the gene encoding the major exosporium protein BclA from the Sterne strain had no significant effect on the LD_{50} in a mouse subcutaneous model of anthrax infection. Additionally, exosporia are found on spores of nonpathogenic species including *B. megaterium* and *Bacillus odysseyi* (45, 85), suggesting that their primary role need not be in disease. Nonetheless, the exosporium may detectably affect spore function. We found that *cotE* mutant spores are more resistant to killing by macrophages, likely as a result of less efficient germination. However, Kang et al. (38) showed that when the exosporium was removed from the Sterne strain by sonication, macrophage killing occurred more readily. Clarification of the role of the exosporium in spore resistance, disease, and maintenance in the environment will be an important future goal. Regardless of its role in the wild, the fact that the exosporium can be removed (mechanically [68] or genetically, as we have done in this work) and that the resulting spores are likely to be suitable for use as a weapon has important implications for the design of future detection, decontamination, and vaccine strategies involving the exosporium (26). Our view is that we should anticipate the potential deployment of spores without exosporia. Therefore, any future antispore vaccine and detection strategies, for example, should include both exosporial as well as coat surface antigens.

ACKNOWLEDGMENTS

We thank Steven Tobery, Kathy Kuehl, Byron Burnette, and Sarah Norris for their assistance with experimental procedures and analysis. We thank Terry Koehler and Tim Hoover for helpful advice and reagents. We thank the Michigan Proteome Consortium for the proteomics data. We especially thank John Kearney for the EG4-4-1 antibody.

This work was conducted in compliance with the Animal Welfare Act and other federal statutes and regulations relating to animals and experiments involving animals and adheres to principles stated in the Guide for the Care and Use of Laboratory Animals, National Research Council, 1996. The facility where this research was conducted is fully accredited by the Association for Assessment and Accreditation of Laboratory Animal Care International.

This work was supported by grants GM53989 and AI53365 from the National Institutes of Health (NIH) (A.D.), grant AI053360 from the NIH (J.R.M.), and the U.S. Army Medical Research and Materiel Command under project numbers 02-4-5C-018 (J.B.), 02-4-5C-023 (S.W.), and 04-0-IL-002 (S.W.).

Opinions, interpretations, conclusions, and recommendations are those of the authors and are not necessarily endorsed by the U.S. Army.

REFERENCES

1. **Aronson, A. I., and P. Fitz-James.** 1976. Structure and morphogenesis of the bacterial spore coat. Bacteriol. Rev. **40:**360–402.
2. **Bagyan, I., and P. Setlow.** 2002. Localization of the cortex lytic enzyme CwlJ in spores of *Bacillus subtilis*. J. Bacteriol. **184:**1219–1224.
3. **Bailey-Smith, K., S. J. Todd, T. W. Southworth, J. Proctor, and A. Moir.** 2005. The ExsA protein of *Bacillus cereus* is required for assembly of coat and exosporium onto the spore surface. J. Bacteriol. **187:**3800–3806.
4. **Bauer, T., S. Little, A. G. Stöver, and A. Driks.** 1999. Functional regions of the *Bacillus subtilis* spore coat morphogenetic protein CotE. J. Bacteriol. **181:**7043–7051.
5. **Berger, J. A., and A. G. Marr.** 1960. Sonic disruption of spores of *Bacillus cereus*. J. Gen. Microbiol. **22:**147–157.
6. **Bowen, W. R., A. S. Fenton, R. W. Lovitt, and C. J. Wright.** 2002. The measurement of *Bacillus mycoides* spore adhesion using atomic force microscopy, simple counting methods, and a spinning disk technique. Biotechnol. Bioeng. **79:**170–179.
7. **Boydston, J. A., L. Yue, J. F. Kearney, and C. L. Turnbough, Jr.** 2006. The ExsY protein is required for complete formation of the exosporium of *Bacillus anthracis*. J. Bacteriol. **188:**7440–7448.
8. **Bozue, J. A., N. Parthasarathy, L. R. Phillips, C. K. Cote, P. F. Fellows, I. Mendelson, A. Shafferman, and A. M. Friedlander.** 2005. Construction of a rhamnose mutation in *Bacillus anthracis* affects adherence to macrophages but not virulence in guinea pigs. Microb. Pathog. **38:**1–12.
9. **Brossier, F., M. Levy, and M. Mock.** 2002. Anthrax spores make an essential contribution to vaccine efficacy. Infect. Immun. **70:**661–664.
10. **Bruno, J. G., and J. L. Kiel.** 1999. In vitro selection of DNA aptamers to anthrax spores with electrochemiluminescence detection. Biosens. Bioelectron. **14:**457–464.
11. **Catalano, F. A., J. Meador-Parton, D. L. Popham, and A. Driks.** 2001. Amino acids in the *Bacillus subtilis* morphogenetic protein SpoIVA with roles in spore coat and cortex formation. J. Bacteriol. **183:**1645–1654.

12. **Chada, V. G., E. A. Sanstad, R. Wang, and A. Driks.** 2003. Morphogenesis of *Bacillus* spore surfaces. J. Bacteriol. **185:**6255–6261.
13. **Cohen, S., I. Mendelson, Z. Altboum, D. Kobiler, E. Elhanany, T. Bino, M. Leitner, I. Inbar, H. Rosenberg, Y. Gozes, R. Barak, M. Fisher, C. Kronman, B. Velan, and A. Shafferman.** 2000. Attenuated nontoxinogenic and nonencapsulated recombinant *Bacillus anthracis* spore vaccines protect against anthrax. Infect. Immun. **68:**4549–4558.
14. **Cutting, S. M., and P. B. Vander Horn.** 1990. Molecular biological methods for *Bacillus*. John Wiley & Sons Ltd., Chichester, United Kingdom.
15. **Dixon, T. C., A. A. Fadl, T. M. Koehler, J. A. Swanson, and P. C. Hanna.** 2000. Early *Bacillus anthracis*-macrophage interactions: intracellular survival and escape. Cell. Microbiol. **2:**453–463.
16. **Driks, A.** 1999. The *Bacillus subtilis* spore coat. Microbiol. Mol. Biol. Rev. **63:**1–20.
17. **Driks, A.** 2003. The dynamic spore. Proc. Natl. Acad. Sci. USA **100:**3007–3009.
18. **Driks, A.** 2002. Maximum shields: the armor plating of the bacterial spore. Trends Microbiol. **10:**251–254.
19. **Driks, A.** 2002. Proteins of the spore core and coat, p. 527–536. *In* A. L. Sonenshein, J. A. Hoch, and R. Losick (ed.), *Bacillus subtilis* and its closest relatives. American Society for Microbiology, Washington, DC.
20. **Driks, A., S. Roels, B. Beall, C. P. J. Moran, and R. Losick.** 1994. Subcellular localization of proteins involved in the assembly of the spore coat of *Bacillus subtilis*. Genes Dev. **8:**234–244.
21. **Driks, A., and P. Setlow.** 2000. Morphogenesis and properties of the bacterial spore, p. 191–218. *In* Y. V. Brun and L. J. Shimkets (ed.), Prokaryotic development. American Society for Microbiology, Washington, DC.
22. **Drysdale, M., S. Heninger, J. Hutt, Y. Chen, C. R. Lyons, and T. M. Koehler.** 2005. Capsule synthesis by *Bacillus anthracis* is required for dissemination in murine inhalation anthrax. EMBO J. **24:**221–227.
23. **Eichenberger, P., M. Fujita, S. T. Jensen, E. M. Conlon, D. Z. Rudner, S. T. Wang, C. Ferguson, K. Haga, T. Sato, J. S. Liu, and R. Losick.** 2004. The program of gene transcription for a single differentiating cell type during sporulation in *Bacillus subtilis*. PLoS Biol. **2:**e328.
24. **Eichenberger, P., S. T. Jensen, E. M. Conlon, C. van Ooij, J. Silvaggi, J. E. Gonzalez-Pastor, M. Fujita, S. Ben-Yehuda, P. Stragier, J. S. Liu, and R. Losick.** 2003. The sigmaE regulon and the identification of additional sporulation genes in *Bacillus subtilis*. J. Mol. Biol. **327:**945–972.
25. **Fotiadis, D., S. Scheuring, S. A. Muller, A. Engel, and D. J. Muller.** 2002. Imaging and manipulation of biological structures with the AFM. Micron **33:**385–397.
26. **Friedlander, A. M., S. L. Welkos, and B. E. Ivins.** 2002. Anthrax vaccines. Curr. Top. Microbiol. Immunol. **271:**33–60.
27. **Gerhardt, P.** 1967. Cytology of *Bacillus anthracis*. Fed. Proc. **26:**1504–1517.
28. **Gerhardt, P., and E. Bibi.** 1964. Ultrastructure of the exosporium enveloping spores of *Bacillus cereus*. J. Bacteriol. **88:**1774–1789.
29. **Gerhardt, P., R. Scherrer, and S. Black.** 1972. Molecular sieving by dormant spore structures, p. 68–74. *In* H. O. Halvorson, R. Hanson, and L. L. Campbell (ed.), Spores V. American Society for Microbiology, Washington, DC.
30. **Green, B. D., L. Battisti, T. M. Koehler, C. B. Thorne, and B. E. Ivins.** 1985. Demonstration of a capsule plasmid in *Bacillus anthracis*. Infect. Immun. **49:**291–297.
31. **Guidi-Rontani, C., M. Levy, H. Ohayon, and M. Mock.** 2001. Fate of germinated *Bacillus anthracis* spores in primary murine macrophages. Mol. Microbiol. **42:**931–938.
32. **Henriques, A. O., T. V. Costa, L. O. Martins, and R. Zilhao.** 2004. The functional architecture and assembly of the coat, p. 65–86. *In* R. E. Ricca, A. O. Henriques, and S. M. Cutting (ed.), Bacterial spore formers: probiotics and emerging applications. Horizon Bioscience, Norfolk, United Kingdom.
33. **Henriques, A. O., and C. P. Moran, Jr.** 2000. Structure and assembly of the bacterial endospore coat. Methods **20:**95–110.
34. **Holt, S. C., and E. R. Leadbetter.** 1969. Comparative ultrastructure of selected aerobic spore-forming bacteria: a freeze-etching study. Bacteriol. Rev. **33:**346–378.
35. **Ivins, B. E., P. F. Fellows, and G. O. Nelson.** 1994. Efficacy of a standard human anthrax vaccine against *Bacillus anthracis* spore challenge in guinea-pigs. Vaccine **12:**872–874.
36. **Ivins, B. E., S. L. Welkos, G. B. Knudson, and S. F. Little.** 1990. Immunization against anthrax with aromatic compound-dependent (Aro^-) mutants of *Bacillus anthracis* and with recombinant strains of *Bacillus subtilis* that produce anthrax protective antigen. Infect. Immun. **58:**303–308.
37. **Johnson, M. J., S. J. Todd, D. A. Ball, A. M. Shepherd, P. Sylvestre, and A. Moir.** ExsY and CotY are required for the correct assembly of the exosporium and spore coat of *Bacillus cereus*. J. Bacteriol. **188:**7905–7913.
38. **Kang, T. J., M. J. Fenton, M. A. Weiner, S. Hibbs, S. Basu, L. Baillie, and A. S. Cross.** 2005. Murine macrophages kill the vegetative form of *Bacillus anthracis*. Infect. Immun. **73:**7495–7501.
39. **Kim, H., M. Hahn, P. Grabowski, D. C. McPherson, R. Wang, C. Ferguson, P. Eichenberger, and A. Driks.** 2006. The *Bacillus subtilis* spore coat protein interaction network. Mol. Microbiol. **59:**487–502.
40. **Kim, H. S., D. Sherman, F. Johnson, and A. I. Aronson.** 2004. Characterization of a major *Bacillus anthracis* spore coat protein and its role in spore inactivation. J. Bacteriol. **186:**2413–2417.
41. **Koehler, T. M., Z. Dai, and M. Kaufman-Yarbray.** 1994. Regulation of the *Bacillus anthracis* protective antigen gene: CO_2 and a *trans*-acting element activate transcription from one of two promoters. J. Bacteriol. **176:**586–595.
42. **Kramer, M. J., and I. L. Roth.** 1968. Ultrastructural differences in the exosporium of the Sterne and Vollum strains of *Bacillus anthracis*. Can. J. Microbiol. **14:**1297–1299.
43. **Kunst, F., N. Ogasawara, I. Moszer, A. M. Albertini, G. Alloni, V. Azevedo, M. G. Bertero, P. Bessières, A. Bolotin, S. Borchert, R. Borriss, L. Boursier, A. Brans, M. Braun, S. C. Brignell, S. Bron, S. Brouillet, C. V. Bruschi, B. Caldwell, V. Capuano, N. M. Carter, S.-K. Choi, J.-J. Codani, I. F. Connerton, et al.** 1997. The complete genome sequence of the gram-positive bacterium *Bacillus subtilis*. Nature **390:**249–256.
44. **Kuwana, R., Y. Kasahara, M. Fujibayashi, H. Takamatsu, N. Ogasawara, and K. Watabe.** 2002. Proteomics characterization of novel spore proteins of *Bacillus subtilis*. Microbiology **148:**3971–3982.
45. **La Duc, M. T., M. Sakomi, and K. Venkateswaran.** 2004. *Bacillus odysseyi* sp. nov., a round-spore-forming bacillus isolated from the Mars Odyssey spacecraft. Int. J. Syst. Evol. Microbiol. **54:**195–201.
46. **Lai, E.-M., N. D. Phadke, M. T. Kachman, R. Giorno, S. Vazquez, J. A. Vazquez, J. R. Maddock, and A. Driks.** 2003. Proteomic analysis of the spore coats of *Bacillus subtilis* and *Bacillus anthracis*. J. Bacteriol. **185:**1443–1454.
47. **Leighton, T. J., and R. H. Doi.** 1971. The stability of messenger ribonucleic acid during sporulation in *Bacillus subtilis*. J. Biol. Chem. **246:**3189–3195.
48. **Little, S., and A. Driks.** 2001. Functional analysis of the *Bacillus subtilis* morphogenetic spore coat protein CotE. Mol. Microbiol. **42:**1107–1120.
49. **Little, S. F., and G. B. Knudson.** 1986. Comparative efficacy of *Bacillus anthracis* live spore vaccine and protective antigen vaccine against anthrax in the guinea pig. Infect. Immun. **52:**509–512.
50. **Liu, H., N. H. Bergman, B. Thomason, S. Shallom, A. Hazen, J. Crossno, D. A. Rasko, J. Ravel, T. D. Read, S. N. Peterson, J. Yates III, and P. C. Hanna.** 2004. Formation and composition of the *Bacillus anthracis* endospore. J. Bacteriol. **186:**164–178.
51. **Lyons, C. R., J. Lovchik, J. Hutt, M. F. Lipscomb, E. Wang, S. Heninger, L. Berliba, and K. Garrison.** 2004. Murine model of pulmonary anthrax: kinetics of dissemination, histopathology, and mouse strain susceptibility. Infect. Immun. **72:**4801–4809.
52. **McPherson, D., H. Kim, M. Hahn, R. Wang, P. Grabowski, P. Eichenberger, and A. Driks.** 2005. Characterization of the *Bacillus subtilis* spore coat morphogenetic protein CotO. J. Bacteriol. **187:**8278–8290.
53. **Mendelson, I., S. Tobery, A. Scorpio, J. Bozue, A. Shafferman, and A. M. Friedlander.** 2004. The NheA component of the non-hemolytic enterotoxin of *Bacillus cereus* is produced by *Bacillus anthracis* but is not required for virulence. Microb. Pathog. **37:**149–154.
54. **Mock, M., and A. Fouet.** 2001. Anthrax. Annu. Rev. Microbiol. **55:**647–671.
55. **Moir, A., B. M. Corfe, and J. Behravan.** 2002. Spore germination. Cell. Mol. Life Sci. **59:**403–409.
56. **Moir, A., and D. A. Smith.** 1990. The genetics of bacterial spore germination. Annu. Rev. Microbiol. **44:**531–553.
57. **Naclerio, G., L. Baccigalupi, R. Zilhao, M. De Felice, and E. Ricca.** 1996. *Bacillus subtilis* spore coat assembly requires *cotH* gene expression. J. Bacteriol. **178:**4375–4380.
58. **Nicholson, W. L.** 2002. Roles of *Bacillus* endospores in the environment. Cell. Mol. Life Sci. **59:**410–416.
59. **Ohye, D. F., and W. G. Murrell.** 1973. Exosporium and spore coat formation in *Bacillus cereus* T. J. Bacteriol. **115:**1179–1190.
60. **Ozin, A. J., A. O. Henriques, H. Yi, and C. P. Moran, Jr.** 2000. Morphogenetic proteins SpoVID and SafA form a complex during assembly of the *Bacillus subtilis* spore coat. J. Bacteriol. **182:**1828–1833.
61. **Paidhungat, M., K. Ragkousi, and P. Setlow.** 2001. Genetic requirements for induction of germination of spores of *Bacillus subtilis* by Ca^{2+}-dipicolinate. J. Bacteriol. **183:**4886–4893.
62. **Perez-Casal, J., M. G. Caparon, and J. R. Scott.** 1991. Mry, a *trans*-acting positive regulator of the M protein gene of *Streptococcus pyogenes* with similarity to the receptor proteins of two-component regulatory systems. J. Bacteriol. **173:**2617–2624.
63. **Piggot, P. J., and J. G. Coote.** 1976. Genetic aspects of bacterial endospore formation. Bacteriol. Rev. **40:**908–962.
64. **Pogliano, K., E. Harry, and R. Losick.** 1995. Visualization of the subcellular location of sporulation proteins in *Bacillus subtilis* using immunofluorescence microscopy. Mol. Microbiol. **18:**459–470.
65. **Price, K. D., and R. Losick.** 1999. A four-dimensional view of assembly of a morphogenetic protein during sporulation in *Bacillus subtilis*. J. Bacteriol. **181:**781–790.
66. **Priest, F. G.** 1993. Systematics and ecology of *Bacillus*, p. 3–16. *In* A. L. Sonenshein, J. Hoch, and R. Losick (ed.), *Bacillus subtilis* and other gram-positive bacteria: biochemistry, physiology, and molecular genetics. American Society for Microbiology, Washington, DC.
67. **Read, T. D., S. N. Peterson, N. Tourasse, L. W. Baillie, I. T. Paulsen, K. E. Nelson, H. Tettelin, D. E. Fouts, J. A. Eisen, S. R. Gill, E. K. Holtzapple, O. A. Okstad, E. Helgason, J. Rilstone, M. Wu, J. F. Kolonay, M. J. Beanan,**

R. J. Dodson, L. M. Brinkac, M. Gwinn, R. T. DeBoy, R. Madpu, S. C. Daugherty, A. S. Durkin, D. H. Haft, W. C. Nelson, J. D. Peterson, M. Pop, H. M. Khouri, D. Radune, J. L. Benton, Y. Mahamoud, L. Jiang, I. R. Hance, J. F. Weidman, K. J. Berry, R. D. Plaut, A. M. Wolf, K. L. Watkins, W. C. Nierman, A. Hazen, R. Cline, C. Redmond, J. E. Thwaite, O. White, S. L. Salzberg, B. Thomason, A. M. Friedlander, T. M. Koehler, P. C. Hanna, A. B. Kolsto, and C. M. Fraser. 2003. The genome sequence of *Bacillus anthracis* Ames and comparison to closely related bacteria. Nature **423:** 81–86.

68. **Redmond, C., L. W. Baillie, S. Hibbs, A. J. Moir, and A. Moir.** 2004. Identification of proteins in the exosporium of *Bacillus anthracis*. Microbiology **150:**355–563.
69. **Rhee, K. J., P. Sethupathi, A. Driks, D. K. Lanning, and K. L. Knight.** 2004. Role of commensal bacteria in development of gut-associated lymphoid tissues and preimmune antibody repertoire. J. Immunol. **172:**1118–1124.
70. **Roels, S., A. Driks, and R. Losick.** 1992. Characterization of *spoIVA*, a sporulation gene involved in coat morphogenesis in *Bacillus subtilis*. J. Bacteriol. **174:**575–585.
71. **Sambrook, J., E. F. Fritsch, and T. Maniatis.** 1989. Molecular cloning: a laboratory manual, 2nd ed. Cold Spring Harbor Laboratory Press, Cold Spring Harbor, NY.
72. **Santo, L. Y., and R. H. Doi.** 1974. Ultrastructural analysis during germination and outgrowth of *Bacillus subtilis* spores. J. Bacteriol. **120:**475–481.
73. **Schaeffer, P., J. Millet, and J. Aubert.** 1965. Catabolite repression of bacterial sporulation. Proc. Natl. Acad. Sci. USA **54:**704–711.
74. **Setlow, P.** 2003. Spore germination. Curr. Opin. Microbiol. **6:**550–556.
75. **Setlow, P.** 2006. Spores of *Bacillus subtilis*: their resistance to and killing by radiation, heat and chemicals. J. Appl. Microbiol. **101:**514–525.
76. **Shao, Z., J. Mou, D. M. Czajkowsky, J. Yang, and J. Y. Yuan.** 1996. Biological atomic force microscopy: what is achieved and what is needed. Adv. Physics **45:**1–86.
77. **Sonenshein, A. L.** 2000. Control of sporulation initiation in *Bacillus subtilis*. Curr. Opin. Microbiol. **3:**561–566.
78. **Steichen, C., P. Chen, J. F. Kearney, and C. L. Turnbough, Jr.** 2003. Identification of the immunodominant protein and other proteins of the *Bacillus anthracis* exosporium. J. Bacteriol. **185:**1903–1910.
79. **Stevens, C. M., R. Daniel, N. Illing, and J. Errington.** 1992. Characterization of a sporulation gene, *spoIVA*, involved in spore coat morphogenesis in *Bacillus subtilis*. J. Bacteriol. **174:**586–594.
80. **Sylvestre, P., E. Couture-Tosi, and M. Mock.** 2002. A collagen-like surface glycoprotein is a structural component of the *Bacillus anthracis* exosporium. Mol. Microbiol. **45:**169–178.
81. **Sylvestre, P., E. Couture-Tosi, and M. Mock.** 2003. Polymorphism in the collagen-like region of the *Bacillus anthracis* BclA protein leads to variation in exosporium filament length. J. Bacteriol. **185:**1555–1563.
82. **Takamatsu, H., T. Kodama, T. Nakayama, and K. Watabe.** 1999. Characterization of the *yrbA* gene of *Bacillus subtilis*, involved in resistance and germination of spores. J. Bacteriol. **181:**4986–4994.
83. **Takamatsu, H., and K. Watabe.** 2002. Assembly and genetics of spore protective structures. Cell. Mol. Life Sci. **59:**434–444.
84. **Turnbough, C. L., Jr.** 2003. Discovery of phage display peptide ligands for species-specific detection of Bacillus spores. J. Microbiol. Methods **53:**263–271.
85. **Vary, P. S.** 1994. Prime time for *Bacillus megaterium*. Microbiology **140:**1001–1013.
86. **Warth, A. D., D. F. Ohye, and W. G. Murrell.** 1963. The composition and structure of bacterial spores. J. Cell Biol. **16:**579–592.
87. **Weiner, M. A., T. D. Read, and P. C. Hanna.** 2003. Identification and characterization of the *gerH* operon of *Bacillus anthracis* endospores: a differential role for purine nucleosides in germination. J. Bacteriol. **185:**1462–1464.
88. **Welkos, S., A. Friedlander, S. Weeks, S. Little, and I. Mendelson.** 2002. *In-vitro* characterization of the phagocytosis and fate of anthrax spores in macrophages and the effects of anti-PA antibody. J. Med. Microbiol. **51:**821–831.
89. **Welkos, S. L., C. K. Cote, K. M. Rea, and P. H. Gibbs.** 2004. A microtiter fluorometric assay to detect the germination of *Bacillus anthracis* spores and the germination inhibitory effects of antibodies. J. Microbiol. Methods **56:** 253–265.
90. **Welkos, S. L., and A. M. Friedlander.** 1988. Pathogenesis and genetic control of resistance to the Sterne strain of *Bacillus anthracis*. Microb. Pathog. **4:**53–69.
91. **Welkos, S. L., R. W. Trotter, D. M. Becker, and G. O. Nelson.** 1989. Resistance to the Sterne strain of *B. anthracis*: phagocytic cell responses of resistant and susceptible mice. Microb. Pathog. **7:**15–35.
92. **Williams, D. D., O. Benedek, and C. L. Turnbough, Jr.** 2003. Species-specific peptide ligands for the detection of *Bacillus anthracis* spores. Appl. Environ. Microbiol. **69:**6288–6293.
93. **Youngman, P., J. B. Perkins, and R. Losick.** 1984. Construction of a cloning site near one end of Tn*917* into which foreign DNA may be inserted without affecting transposition in *Bacillus subtilis* or expression of the transposon-borne *erm* gene. Plasmid **12:**1–9.
94. **Zheng, L., W. P. Donovan, P. C. Fitz-James, and R. Losick.** 1988. Gene encoding a morphogenic protein required in the assembly of the outer coat of the *Bacillus subtilis* endospore. Genes Dev. **2:**1047–1054.
95. **Zilhao, R., G. Naclerio, A. O. Henriques, L. Baccigalupi, C. P. Moran, Jr., and E. Ricca.** 1999. Assembly requirements and role of CotH during spore coat formation in *Bacillus subtilis*. J. Bacteriol. **181:**2631–2633.